

CT Characteristics of a Transplantable Canine Glioma Model: Preliminary Kinetic Analysis

Michael Salcman,¹ Krishna C. V. G. Rao, Eric W. Scott, Edwin H. Bellis, and Otis R. Blaumanis

Experimental brain tumors can be produced in dogs through the intracerebral injection of 3×10^6 live tumor cells in either neonates or adult animals. Tumors are visible by computed tomography on day 8 postinjection. Most tumors appear as ring lesions with central lucencies and shaggy borders. By postinjection day 12, tumor volumes increase more than 10 times; the cell cycling time is about 1–3 days. The initial doubling time is about 1–2 days and corresponds to the *in vitro* doubling time of about 24 hr. The use of computed tomography to perform non-invasive kinetic analysis deserves further study. The transplantable canine glioma model would appear to be ideal for this purpose.

Experimental brain tumors can be produced in dogs through the intracerebral injection of either live avian sarcoma virus or a suspension of live tumor cells harvested from other animals. In both neonatal and adult dogs such tumors have been successfully imaged through the use of computed tomography (CT) [1, 2]. In addition to the relatively large size of the animal preparation, the transplantable canine glioma model has the advantage of rapid and reliable induction so that the expectation of visible tumor on CT is usually fulfilled by a specific postinjection interval. In large animal models, surgical manipulation and pharmacologic investigations are facilitated. Sequential CT scanning can be used to study the effects of therapeutic intervention in a manner similar to that employed in clinical trials [3]. In addition to purely morphologic information, there is the distinct possibility that sequential CT scanning will yield noninvasive information concerning the growth characteristics and kinetic properties of tumors. Yamashita [4] has provided formulas by which such estimations can be carried out and has described preliminary results based on an analysis of human tumors. We recently adapted the transplantable canine glioma model to tissue culture. Purified suspensions of such cells cause rapid growth of tumors in adult dogs. It would seem logical that a reliable large animal model with well-defined *in vitro* growth characteristics would provide the ideal means by which to study the feasibility of noninvasive kinetic analysis. This report represents our preliminary attempt to correlate the behavior of the transplantable canine glioma by CT with results obtained by other methods.

Materials and Methods

Frozen tumor brei harvested from previously injected neonatal mongrels was grown in tissue culture using RPMI 1640 with 10% fetal calf serum in 75 cm² tissue culture flasks. The cells were

incubated at 37°C in an atmosphere with 5% CO₂. Before confluence was reached cells were disaggregated with trypsin-ETDA, washed with Hanks balanced salt solution, and spun down into injection volumes of 0.1 ml. Before inoculation, tumor cell viability was determined with trypan blue exclusion and cell counts were made by hemocytometer. Inoculation doses ranged from 3×10^6 to 10×10^6 cells and viability was at least 90%–95% in all cases. Full details of the *in vitro* characterization of the transplantable canine glioma model will be presented in another publication (Bellis et al., in preparation). Two puppies were hand-injected on day 1 of life according to our previously described technique [2]. Three adult mongrel dogs weighing 15–25 kg were anesthetized with 50 mg/kg of ketamine and injected with tumor through a twist drill hole over the left frontoparietal region.

Animals were scanned on either a model O450 Pfizer body scanner or on a GE 8800. Neonatal dogs were sedated with intraperitoneal pentobarbital and placed in a specially designed plexiglass scanning chamber [2]. Adult dogs were premedicated with chlorpromazine and atropine sulfate and sedated with intramuscular ketamine and intravenous sodium pentobarbital. They were placed in the prone position with the head extended onto a plastic head rest and laterally immobilized by foam rubber blocks. After a lateral scout film, 5-mm-thick coronal scans were obtained with 3 mm overlap between contiguous cuts. All animals were enhanced with 4 ml/kg of intravenous diatrizoate meglumine (60%). After scanning, some animals were injected with Evans blue and then sacrificed with barbiturate; others were perfused through the heart for either light or electron microscopy [2].

Sequential volumetric measurements were made on the basis of a simple spherical or ellipsoidal approximation of the tumor shape. As we were interested only in an order-of-magnitude determination, it was not considered necessary to use more precise approximations, such as the Simpson rule [5].

Results

All tumors detected by CT were confirmed at autopsy. There was a strong correlation between the radiographic appearance and that observed on cut section, especially in regard to the size and shape of the tumor as well as the presence of areas of hemorrhage and necrosis. Areas of contrast enhancement corresponded to regions of Evans blue dye penetration at postmortem. Electron microscopic abnormalities of the tumor vessels were also observed [2]. Tumors became visible by CT as early as postinjection day 8 and usually produced significant neurologic deficits by postinjection day 12. Adult animals demonstrated hemiparesis, hemianopsia, and sei-

¹All authors: Neuro-Oncology Service, Division of Neurological Surgery, Division of Neuroradiology, and Department of Neurology, University of Maryland Hospital, 22 South Greene Street, Baltimore, MD 21201. Address reprint requests to M. Salcman.

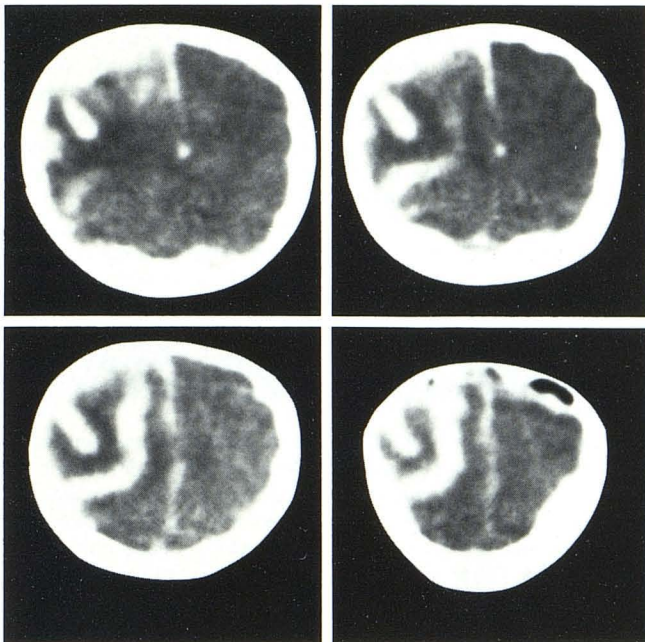


Fig. 1.—Contrast-enhanced coronal CT scans of adult dog, postinjection day 12.

zures. Tumors often appeared as irregular ring lesions with lucent centers and shaggy margins (fig. 1). Peritumoral edema was obvious, and displacement of the falx and the ventricles was easily detected. Tumor growth in the subdural and subgaleal spaces was also demonstrated by CT, and presumably occurred as a result of reflux along the injection track. There was no correlation between the final volume of the tumor and the number of cells initially injected. One adult animal that failed to grow tumors was negative by CT scan on two separate occasions.

At seven points in time it was possible to measure the major and minor axes of the tumor as they appeared on the CT slice of greatest cross-sectional area. Estimates of the volume of the tumor were then made by assuming either a spherical or an ellipsoidal geometry for the lesions. In the case of the latter, a range of values was obtained by using either the major or the minor axis twice, that is, $V = \frac{1}{6}(abc)$, and the remaining axis once. Such values for the volume of the tumor were intermediate in magnitude when compared with spherical approximations utilizing only the major or minor axis. On postinjection days 9 and 10, estimates of the tumor volume in the two puppies were in the range of 1.34–2.14 cm³. In the three adults, on postinjection days 12 and 13 the volume estimates were in the range of 2.92–7.42 cm³. In all animals, therefore, the original injection volume of 0.1 cm³ had increased by more than $\times 10$ but less than a factor of 100.

As indicated by Yamashita, it is possible to estimate the cell cycle time of a tumor employing the formula:

$$T_c = \frac{\log(1 + GF)}{\log(V_b/V_a)} \times t,$$

where T_c is the cell cycle time in days, GF is the growth fraction, V_b/V_a is the ratio of two estimates of the tumor volume, and t is the interval in days between the two estimates. Figure 2 presents the results of a parametric analysis in which T_c is plotted over the entire range of possible values for GF (i.e., 0.05–1.0). Assuming only that the interval between the two measurements of V is 12 days, it is apparent that the true value of T_c must lie between the two curves

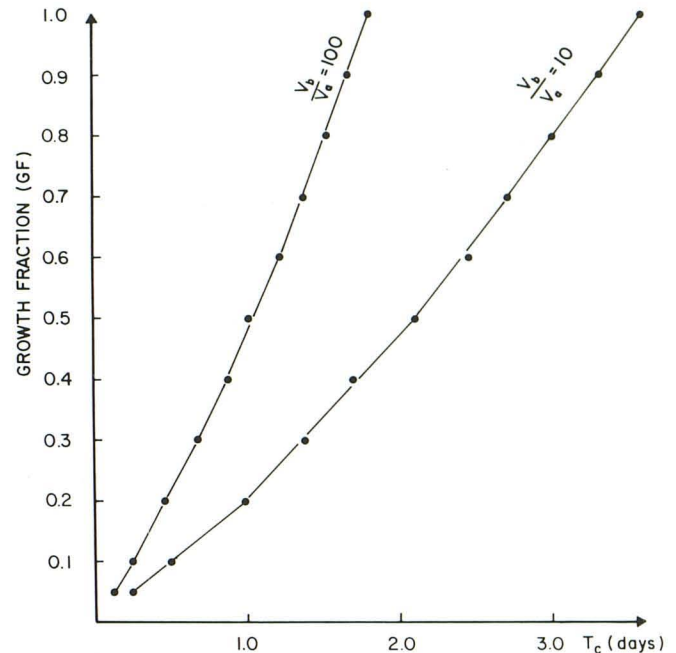


Fig. 2.—Computed cell cycle times (T_c) for $\times 10$ increase ($V_b/V_a = 10$) and $\times 100$ increase ($V_b/V_a = 100$) in tumor volume plotted against all possible growth fractions (GF). As all observed V_b/V_a have fallen between these values, it is assumed T_c for any given GF falls between these two curves.

for any volumetric change greater than 10 and less than 100. This value is on the order of 1–3 days.

The rapid growth of the tumor is graphically illustrated in figures 3 and 4, where growth curves are presented for both the spherical (S) and ellipsoidal (E) estimates of the sequential tumor volume in a single animal. Over the short interval of 4 days, sequential scanning yielded estimates for T_c of 1.4–2.2 days at a GF of 0.2, and of 4.5–7 days at a GF of 0.8. These calculations indicate the extreme sensitivity of kinetic estimates in regard to the time of observation and its relation to the total growth history of the tumor. Therefore, our calculations, based on a limited number of observations, must be regarded as preliminary in nature.

It should be noted, however, that sequential CT scanning can also be used to provide estimates of the tumor doubling time (T_d) and that such estimates require no assumptions concerning the growth fraction at the time of observation. The appropriate formula is:

$$T_d = \frac{\log 2}{\log(V_b/V_a)} \times t,$$

where T_d is in days and the other parameters are as before. In the example illustrated in figure 4, T_d is on the order of 5–8 days at 8–12 days after injection. Clearly, the growth of the tumor before day 8 is much more rapid, and T_d is on the order of 1.6–1.9 days.

Discussion

Although an experimental brain tumor has been successfully imaged in the rat [6], the relatively small size of the animal precludes many surgical and pharmacologic manipulations as well as successful kinetic estimation based on sharply demarcated images of the tumor. The transplantable canine glioma model shares several histologic and radiographic features with human brain tumors, and

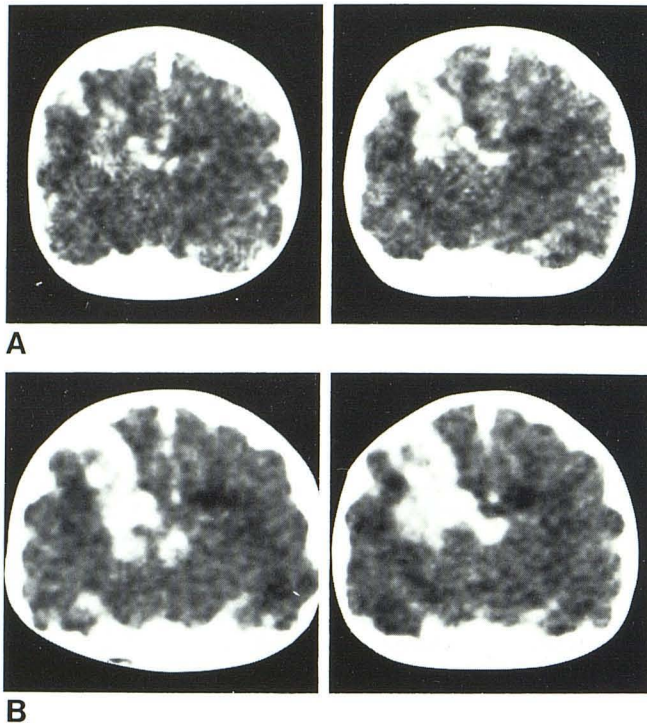


Fig. 3.—Contrast-enhanced coronal CT scans of adult dog, postinjection days 8 (A) and 12 (B). Note increase in tumor size from first study to second, and deformation of left lateral ventricle in both.

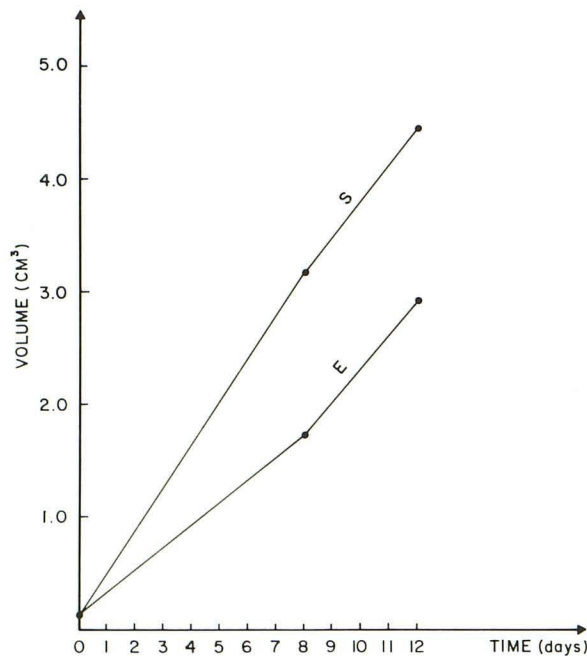


Fig. 4.—Using measurements from CT scans on days 8 and 12, tumor volumes in single animal were calculated using spherical (S) and ellipsoidal (E) approximations. Initial tumor volume was 0.1 cm^3 .

it can be produced in both neonatal and adult dogs [2]. A CT atlas of the canine brain has been prepared and quantitative evaluation of densitometry has already been carried out in this species [7, 8]. Techniques for CT-guided stereotaxy in the dog are being developed in several laboratories [9]. Although similar studies can be carried out in primates, tumor induction is unreliable, the animals are expensive, and the technique involves the use of live virus [10]. In contrast, more than 90% of neonatal mongrels injected with rewarmed tumor brei go on to develop brain tumors, and an equal percentage of adult animals injected with cultured tumor cells also develop intracerebral neoplasms [2]. In both young and old animals, tumors are usually detected by CT as early as postinjection day 8 and frequently develop into typical ring lesions. The animals can be sequentially scanned, either to determine the response of the tumor to therapy or to test hypotheses concerning the growth characteristics of the lesion [3, 4].

In this paper, we have illustrated the ability to use sequential scanning in an attempt to estimate the cell cycle and tumor doubling times of a model brain tumor. The results obtained clearly indicate that a purified and highly viable suspension of tumor cells can produce in vivo growth rates that are similar to those obtained in tissue culture. The in vitro tumor doubling time of the canine glioma model is about 24 hr. This agrees well with the value of 1.6–1.9 days obtained by CT scanning in the live animal. Nevertheless, these data are preliminary in nature and much more will need to be done before noninvasive kinetic analysis becomes a useful tool in the clinical and laboratory study of glial tumors.

REFERENCES

- Groothuis DR, Mikhael MA, Fischer JM, et al. Computed tomography of virally induced canine brain tumors: a preliminary report. *J Comput Assist Tomogr* 1981;5:538–543
- Salcman M, Scott EW, Schepp RS, Knipp HC, Broadwell RD. Transplantable canine glioma model for use in experimental neuro-oncology. *Neurosurgery* 1982;11:372–381
- Salcman M, Levine H, Rao K. Value of sequential computed tomography in the multimodality treatment of glioblastoma multiforme. *Neurosurgery* 1981;8:15–19
- Yamashita T. Estimation of the growth rate of malignant gliomas by CT scanning. Calculation of the actual tumor doubling times and clinical application of the growth rate of malignant gliomas. *Yokohama Medical J* 1981;32:469–479
- Brenner DE, Whitley NO, Houk TL, Aisner J, Wiernik P, Whitley J. Volume determinations in computed tomography. *JAMA* 1982;247:1299–1302
- Kapp JP, Holla PS. Detection of experimental brain tumor in rat by computed tomography. *Surg Neurol* 1981;16:455–458
- Kaufman HH, Cohen G, Glass TF, et al. CT atlas of the dog brain. *J Comput Assist Tomogr* 1981;5:529–537
- Fike JR, Cann CE, Berninger WH. Quantitative evaluation of the canine brain using computed tomography. *J Comput Assist Tomogr* 1982;6:325–333
- Ostertag CB, Weigel K. Three-dimensional CT scanning of the dog brain. *J Comput Assist Tomogr* 1982;6:1036–1037
- Rieth JG, Di Chiro G, London WT, et al. Experimental glioma in primates: a computed tomography model. *J Comput Assist Tomogr* 1980;4:285–290